On the Effective Differentiation and Monitoring of Variable Degrees of Hyperbilirubinemia Severity Through Noninvasive Screening Protocols

Gladimir V. G. Baranoski[1], Senior Member, IEEE, Tenn F. Chen[2] and Petri Varsa[1]

***Abstract*— The presence of abnormal amounts of bilirubin in the blood stream and skin, usually referred to as hyperbilirubinemia, is associated with a wide range of pathologies that can pose considerable risks for human health. The early and effective screening of the severity degrees of this medical condition can play an important role on the selection of the appropriate treatment for the associated pathologies. This, in turn, can minimize the need for more aggressive and costly therapeutic interventions which can themselves pose considerable risks for morbidity and mortality. The current noninvasive protocols used to differentiate these severity degrees, however, are hindered by the relatively limited knowledge about the impact of different amounts of extravascular bilirubin on skin spectral responses and on the onset of jaundice, the resulting yellow-tinted skin appearance. In this paper, we address this open problem through controlled *in silico* experiments supported by measured data provided in the related literature. Our experimental findings bring biophysically-based insights to bear on the clarification of this biomedical entanglement, and unveil optical features that can potentially lead to more effective screening protocols for the noninvasive differentiation and monitoring of variable degrees of hyperbilirubinemia severity.**

***Index Terms*— bilirubin, skin, spectral reflectance, hyperbilirubinemia, jaundice, screening, *in silico* experiments.**

I. Introduction

Human blood is composed primarily of erythrocytes (red blood cells containing hemoglobin) suspended in plasma [1]. When aging erythrocytes are removed from circulation, the breakdown of hemoglobin results in byproducts, notably bilirubin [2]. This pigment binds with albumin, a protein found in plasma, forming a compound known as unconjugated bilirubin (UCB), which is not water soluble. Under normal conditions, this compound is cleared from the blood stream by the liver, where it is conjugated (chemically bound to glucuronic acid) to form water soluble metabolites that are secreted into the bile [2], [3].

Unconjugated (indirect) hyperbilirubinemia develops when the hemoglobin breakdown is accelerated and/or hepatic activity is reduced, while conjugated (direct) hyperbilirubinemia occurs when the secretion of bilirubin by the liver is impaired or the bile flow is obstructed [3]. Although conjugated hyperbilirubinemia is considered innocuous [3], severe degrees of unconjugated hyperbilirubinemia can result in different forms of bilirubin encephalopathy, including irreversible brain damage (kernicterus), in newborns [4], [5], and pigment gallstones in adults [2], [3]. On the other hand, mild degrees of unconjugated hyperbilirubinemia are often associated with benign inherited syndromes, which do not require immediate treatment [3], [6], and may play a protective role against cardiovascular diseases and tumour development [2], [3].

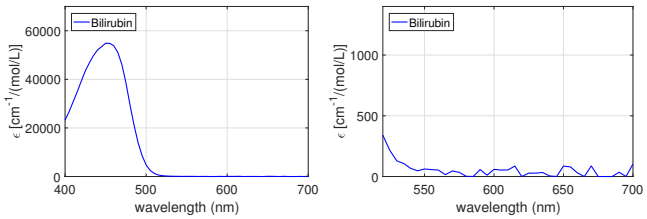

Fig. 1. Bilirubin absorption spectrum. Left: molar extinction coefficient (ε_m) curve [11], [12]. Right: zoom-in plot of the curve on the left.

Within human skin, bilirubin can be found inside and/or outside dermal blood vessels [5], [7]. Although there are still many unknowns in this area, two main mechanisms have been reported as responsible for the presence of this pigment within the cutaneous tissues: deposition of excessive amounts of bilirubin acid from plasma into phospholipid membranes and transference of UCB from plasma into extravascular spaces [8], [9]. In the latter case, experimental evidence indicates that UCB binds with the tissues' constituents [10].

The presence of bilirubin within the cutaneous tissues may lead to noticeable changes in the skin reflectance [13]. These changes are particularly significant in the blue-region (400 to 500 nm) of visible light spectrum due to the absorption peak of bilirubin in this region [2] (Fig. 1 left). Accordingly, they can elicit a yellow-tinted skin appearance commonly referred to as jaundice (icterous) [9], [14], which has been more prominently reported in association with the cutaneous binding of UCB [10].

Standard methods for the detection of unconjugated hyperbilirubinemia rely on the measurement of bilirubin levels in blood samples or in serum (plasma without clotting elements like fibrinogen [1]) using photometric devices [15]. These invasive methods are not only painful and costly, but may also lead to significant blood loss if multiple blood samplings are required, which may be particularly worrisome for preterm infants [16].

The onset of jaundice has also been employed in the clinical estimation of serum bilirubin through the Kramer method [17]. Although such an estimation based on the visual inspection of the affected skin has a lower cost in comparison with invasive methods, it has a markedly lower

*This work was supported in part by the Natural Sciences and Research Council of Canada (NSERC) under Grant 238337.

[1] Gladimir V. G. Baranoski and Petri Varsa are with the Natural Phenomena Simulation Group, School of Computer Science, University of Waterloo, 200 University Avenue, Waterloo, Ontario, N2L 3G1, Canada. gvgbaran@cs.uwaterloo.ca

[2] Tenn F. Chen is with Google Inc., 1600 Amphitheatre Pkwy, Mountain View, CA 94043, USA.

predictive capability [17].

In order to overcome the limitations of invasive methods and visual inspection approaches, different devices have been proposed for the noninvasive transcutaneous measurement of UCB levels associated with changes on skin reflectance [15], [18]. However, the reliability of the measurements provided by these devices is still inferior to the reliability of the measurements obtained through invasive procedures, especially when dealing with high degrees of unconjugated hyperbilirubinemia severity [19], [16], [20].

The major obstacles in this area result from the fact that the processes that regulate the supply and clearance of extravascular UCB are still not completely understood [8], [9], [17] and, thus, not quite predictable [18]. In studies involving the impact of UCB on skin reflectance, usually only the presence of extravascular UCB in the dermal layers is taken into account (*i.e.*, its presence in the outermost skin layer, the stratum corneum, and the epidermal layers [7], [10] is not considered) and/or its quantification is provided as a constant fraction of the intravascular UCB [18], [21].

In this paper, we investigate the impact of different amounts of extravascular bilirubin on skin reflectance. Our findings are expected to directly contribute to the development of more effective screening protocols for the noninvasive differentiation of variable degrees of hyperbilirubinemia severity. Such screening protocols are essential for minimizing the number of unnecessary, costly and potentially risky invasive procedures required to rule out life-threatening conditions such as liver and hematological disorders [3], [6], [22]. Moreover, since the onset of jaundice is still often employed in clinical settings as a visual indicator of the possibility of an imminent emergence of such medical conditions [6], [17], we also assess the reliability of these visual assessments with respect to variations on extravascular bilirubin contents.

II. In Silico Experimental Setup

In this investigation, we used a first-principles model of light and skin interactions, known as HyLIoS (*H*yperspectral *L*ight *I*mpingement on *S*kin) [23], to compute directional-hemispherical reflectance curves for cutaneous tissues containing different amounts of bilirubin. We note that the radiometric predictions provided by this model have been extensively evaluated through comparisons of its outcomes with actual measured data [23] and employed in a wide range of biomedical investigations (*e.g.*, [24], [25], [26]).

Within the HyLIoS' geometrical-optics formulation, a ray interacting with a given skin specimen can be associated with any wavelength within a spectral region of interest. For consistency, we considered a spectral resolution of 5 nm in all curves depicted in this work, which were computed using a virtual spectrophotometer [27]. In their computation, we considered an angle of incidence of 45° and employed 10^6 sample rays. To enable the full reproduction of our *in silico* experimental results, we made HyLIoS available on online [28], [29] along with the supporting biophysical datasets [30] (*e.g.*, refractive index and extinction coefficient curves) used in our investigation.

TABLE I

Parameters employed in the characterization of the skin specimen considered in this investigation. The acronyms SC, SG, SS, SB, PD and RD refer to its main layers: stratum corneum, stratum granulosum, stratum spinosum, stratum basale, papillary dermis and reticular dermis, respectively.

Parameter	Value
Aspect Ratio of Skin Surface Folds	0.1
SC Thickness (cm)	0.001
SG Thickness (cm)	0.0011
SS Thickness (cm)	0.0011
SB Thickness (cm)	0.0011
PD Thickness (cm)	0.04
RD Thickness (cm)	0.1
SC Melanosome Content (%)	0.0
SG Melanosome Content (%)	0.8
SS Melanosome Content (%)	0.8
SB Melanosome Content (%)	0.8
SC Colloidal Melanin Content (%)	0.0
SG Colloidal Melanin Content (%)	3.9
SS Colloidal Melanin Content (%)	3.9
SB Colloidal Melanin Content (%)	3.9
Melanosome Eumelanin Concentration (g/L)	50.0
Melanosome Pheomelanin Concentration (g/L)	2.0
PD Blood Content (%)	0.2
RD Blood Content (%)	0.2
Dermal Oxyhemoglobin Fraction (%)	75
Functional Hemoglobin Concentration in Blood (g/L)	130.0
Methemoglobin Concentration in Blood (g/L)	1.5
Carboxyhemoglobin Concentration in Blood (g/L)	1.5
Sulfhemoglobin Concentration Blood (g/L)	0.0
Blood Bilirubin Concentration (g/L)	0.003
SC Beta-Carotene Concentration (g/L)	2.1E-4
Epidermis Beta-Carotene Concentration (g/L)	2.1E-4
Blood Beta-Carotene Concentration (g/L)	7.0E-5
SC Water Content (%)	35.0
Epidermis Water Content (%)	60.0
PD Water Content (%)	75.0
RD Water Content (%)	75.0
SC Lipid Content (%)	20.0
Epidermis Lipid Content (%)	15.1
PD Lipid Content (%)	17.33
RD Lipid Content (%)	17.33
SC Keratin Content (%)	65.0
SC Urocanic Acid Density (mol/L)	0.01
Skin DNA Density (g/L)	0.185
SC Refractive Index	1.55
Epidermis Refractive Index	1.4
PD Refractive Index	1.39
RD Refractive Index	1.41
Melanin Refractive Index	1.7
PD Scatterers Refractive Index	1.5
Radius of PD Scatterers (nm)	70.0
PD Fraction Occupied by Scatterers (%)	22.0

The parameters used to characterize the cutaneous tissues considered in this investigation are provided in Table I. The selection of values for these parameters was based on their respective physiologically ranges provided in the related literature. These works, unless otherwise cited below, are listed elsewhere [25] for conciseness. Using this dataset, we computed a baseline reflectance curve in close agreement (Fig. 2 (top right)) with a measured reflectance curve [31] employed as a reference. This reference curve was measured by Vrhel et al. [31] on the side of a lightly-pigmented subject's face considering an angle of incidence of 45°. It is

worth noting that neonatal jaundice is first apparent over the newborns' face [10].

Although most of the literature on unconjugated hyperbilirubinemia is directed toward its assessment in neonatal patients, which may be explained by its high incidence (about 60%) in newborns [10], [16], [19], one cannot overlook its medical implications for the adult population [3], [6], [20]. For this reason, whenever possible, we selected parameter values that could be used to characterize both newborn and adult subjects (*e.g.*, the hemoglobin concentration equal to 130 g/L [32] and the radius of reticular dermis scatterers equal to 70 nm [33].).

In our *in silico* experiments, we considered intravascular bilirubin concentrations (denoted by c_{blood}^{bil}) derived from total serum bilirubin (TSB) values reported in the literature for normal (baseline), significant (associated with noticeable signs of bilirubin toxicity), excessive (associated with potentially irreversible bilirubin-induced physiological damages) and extreme (associated with high risks of mortality) levels of bilirubin present in the blood stream: 0.0062 [3], 0.129 [34], 0.292 [4] and 0.419 g/L [4], respectively.

These TSB values were then multiplied by 0.55 to obtain the corresponding c_{blood}^{bil} values: 0003, 0.071, 0.161 and 0.223 g/L, respectively. This operation was necessary since plasma typically accounts for only 55% of the blood volume, with the cellular portion of blood, which is mostly (99%) formed by the erythrocytes [35], accounting for the remaining 45% [1]. The extravascular skin contents of bilirubin were estimated by multiplying the c_{blood}^{bil} values listed above by selected bilirubin transference factors (denoted by f_{skin}^{bil}) employed to account for variable bilirubin acid deposition and albumin-biliribin complex transfer rates [5], [8], [9].

In order to assess the visual impact of distinct degrees of hyperbilirubinemia severity, we generated skin swatches. Their chromatic attributes were obtained from the convolution of a selected illuminant's relative spectral power distribution, the modeled reflectance data and the broad spectral response of the human photoreceptors [36]. This last step was performed by employing a standard CIEXYZ to sRGB color system conversion procedure [37] and considering the CIE D65 illuminant [36] (Fig. 2 (top left)). After computing the chromatic attributes of a swatch, we applied a greyscale texture (Fig. 2 (bottom left)) to make its depiction more realistic. For comparison purposes, we provide the skin swatch (Fig. 2 (bottom right)) obtained using the baseline reflectance curve (Fig. 2 (top right)) computed for the selected specimen.

Besides visual inspection, we also employed a device-independent CIE-based metric to compare skin swatches associated with distinct degrees of hyperbilirubinemia severity. More specifically, we computed the CIELAB differences between pairs of swatches using the following formula [38]:

$$\Delta E_{ab}^{*} = \sqrt{({d_L}^2 + {d_a}^2 + {d_b}^2)}, \tag{1}$$

where d_L, d_a and d_b represent the differences $L_1^* - L_2^*$, $a_1^* - a_2^*$ and $b_1^* - b_2^*$, respectively, in which L^*, a^* and b^* correspond the CIELAB color space dimensions. These are

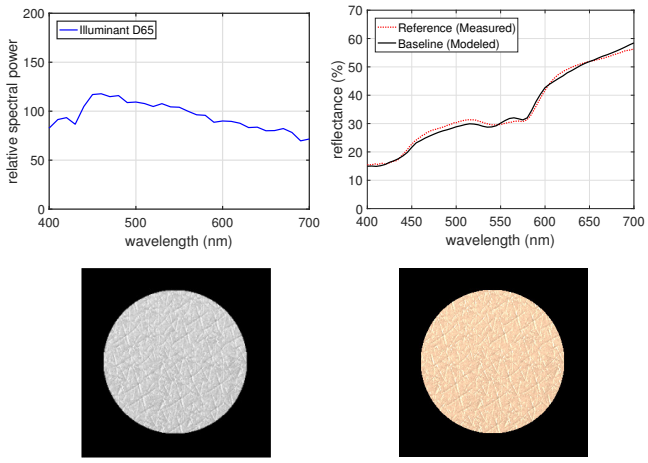

Fig. 2. Components of a convolution process employed to generate a skin swatch for the specimen (baseline) characterized by the parameter values presented in Table I. Top left: relative spectral power distribution of the CIE standard D65 (daylight) illuminant [36]. Top right: reference (measured by Vrhel et al. [31]) and baseline (computed using HyLIoS [28]) reflectance curves. Bottom left: greyscale texture. Bottom right: resulting swatch generated for the baseline reflectance curve.

calculated for the modeled chromatic attributes associated with the compared swatches (indicated by the subscripts 1 and 2, respectively). Again, we performed these calculations using standard formulas employed in colorimetry [39] and considering the CIE D65 illuminant [36].

III. Results and Discussion

Initially, we compute reflectance curves considering only variations in intravascular bilirubin contents ($f_{skin}^{bil} = 0$). As it can be observed in the graph depicted in Fig. 3 (left), the resulting reflectances changes were negligible, thus agreeing with the premise [8], [9], [10] that noticeable changes in skin spectral responses resulting from hyperbilirubinemia are mainly associated with the presence of extravascular bilirubin. In fact, when we took the extravascular bilirubin contents into account ($f_{skin}^{bil} \neq 0$), the resulting reflectance curves exhibited noticeable changes as it can be observed in the graph depicted in Fig. 3 (right). More specifically, as the presence of extravascular bilirubin increases, the reflectance decreases in the blue-region of the light spectrum, with the curve segments in this region going from a concave down to increasingly accentuated concave up shapes. These observations qualitatively agree with reflectance measurements performed by Hannemann *et al.* [13] on lightly-pigmented individuals subjected to distinct degrees of hyperbilirubinemia severity. It is worth noting that devices used in transcutaneous bilirubinometry [19] employ reflectance readings taken in the blue region. Hence, as the differences between the curves become smaller in this region due to an increased presence of extravascular bilirubin increases, one should expect the efficacy of these devices to be diminished accordingly [19].

In Fig. 4, we present the skin swatches obtained considering the modeled reflectance curves depicted in Fig. 3 (right). In these swatches, one can observe a transition to a more noticeable yellow-tinted skin appearance, in comparison with

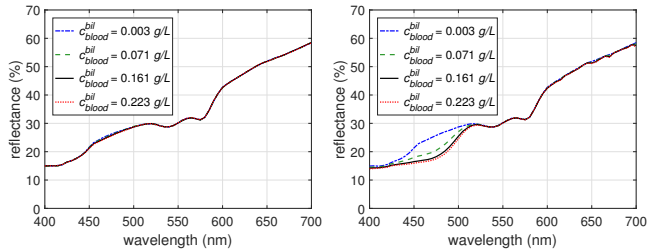

Fig. 3. Graphs depicting reflectance changes due to variations in intravascular and extravascular bilirubin contents, with the former denoted by c^{bil}_{blood} and the latter given by the product of f^{bil}_{skin} (bilirubin transference factor) by c^{bil}_{blood}. Left: $f^{bil}_{skin} = 0$. Right: $f^{bil}_{skin} = 0.05$.

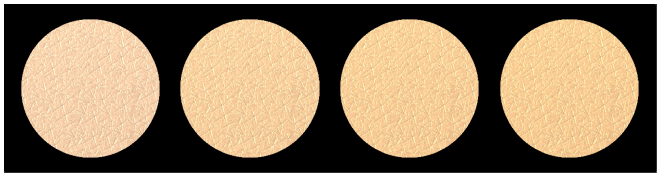

Fig. 4. Skin swatches obtained using the reflectance curves provided in Fig. 3 (right). From left to right, c^{bil}_{blood} varies from 0.003, 0.071, 0.161 and 0.223 g/L, respectively.

the baseline swatch depicted in Fig. 2 (bottom right), as the amount of extravascular bilirubin increases. This aspect is corroborated by the CIELAB ΔE^*_{ab} differences computed for these swatches with respect to the baseline swatch presented in Fig. 2 (bottom right): 0.51, 6.38, 9.71 and 10.92 (from the leftmost to the rightmost swatch). However, as the presence of extravascular bilirubin increases, denoting higher degrees of hyperbilirubinemia severity, the CIELAB ΔE^*_{ab} differences computed for successive pairs of swatches, namely 6.66, 3.33 and 1.22 (from the leftmost to the rightmost pair), decrease substantially. In fact, for the last pair, the difference is smaller than 2.3, the experimentally-determined perceptibility threshold for CIELAB chromatic differences [38], [40].

These aspects indicate that, although a jaundice skin appearance may be of use (under certain favourable conditions with respect to the incident illumination and the subject's skin pigmentation [8], [17]) in the detection of hyperbilirubinemic states, it has limited applicability in the differentiation and monitoring of variable degrees of hyperbilirubinemia severity. This becomes particularly evident when they are associated with excessively high levels of extravascular bilirubin.

In Fig. 5, we present reflectance graphs obtained by simultaneously varying the intravascular and extravascular bilirubin contents. Again, it can be observed that variations in extravascular bilirubin contents have a much larger impact on the resulting reflectance curves. The combined effect resulting from increasing both the intravascular bilirubin content and the fraction of intravascular bilirubin transferred to the surrounding cutaneous tissues is a substantial increase in the extravascular bilirubin content. This, in turn, has two consequences. First, it accentuates the concavity down of the curve segments in the blue region of the light spectrum. Second, it prompts reflectance variations in the red-region (600 to 700 nm) of the light spectrum.

Recall that the absorption spectrum of bilirubin is characterized by a strong peak in the blue region (Fig. 1 (left)) and significantly less pronounced peaks in the red region (Fig. 1 (right)). Although the latter have negligible effects on skin reflectance under normal or less severe hyperbilirubinemic states, they tend to have a noticeable influence, notably around 650 nm, when the presence of extravascular bilirubin reaches considerably high levels. We note that similar reflectance variations around 650 nm can also be observed in the reflectance measurements performed by Hannemann *et al.* [13] on lightly-pigmented individuals subjected to distinct degrees of hyperbilirubinemia severity.

In Fig. 6, we present the skin swatches obtained considering the modeled reflectance curves depicted in Fig. 5. Again, in these swatches, one can observe a transition to a more noticeable yellow-tinted skin appearance, in comparison with the baseline swatch depicted in Fig. 2 (bottom right), as the amount of extravascular bilirubin increases. This aspect is also corroborated by the CIELAB ΔE^*_{ab} differences computed for these swatches. For example, the difference computed for the swatch placed at the bottom right corner of the grid with respect to the baseline swatch presented in Fig. 2 (bottom right) is 12.14. However, as the presence of extravascular bilirubin increases, denoting higher degrees of hyperbilirubinemia severity, the CIELAB ΔE^*_{ab} differences computed for neighbour swatches tend to become smaller as the amount of extravascular bilirubin increases. For example, the difference computed for the swatch placed at the bottom right corner of the grid with respect to the swatch placed just above it is 1.23. This value is considerably lower than the experimentally-determined perceptibility threshold (2.3) for CIELAB chromatic differences [38], [40]. Once again, this aspect illustrates the limited applicability of visual assessments of subjects' jaundice when comes to the differentiation and monitoring of variable degrees of hyperbilirubinemia severity associated with excessively high levels of extravascular bilirubin.

Clearly, the difficulties in differentiating variable degrees of hyperbilirubinemia severity, namely the relative proximity of the resulting reflectance curves in the blue region and the absence of distinguishable differences between the associated yellow-tinted skin appearances, are exacerbated as the extravascular bilirubin contents increase. Ideally, for completeness, we would like to perform experiments considering a tight upper bound for f^{bil}_{skin}. However, due to the largely unpredictable processes that regulate the transference of bilirubin from blood to skin extravascular spaces (and vice-versa) [9], [18], experimental studies in this area still lack quantitative data required for the specification of this bound. For this reason, we considered a putative value ($f^{bil}_{skin} = 0.2$) employed in a related work [21]. The observations derived from our experiments considering this value were qualitatively the same as those derived from our previous experiments. More specifically, as it can be observed in the graph presented in Fig. 7 (left), the reflectance curves exhibit smaller differences between each other in the blue region

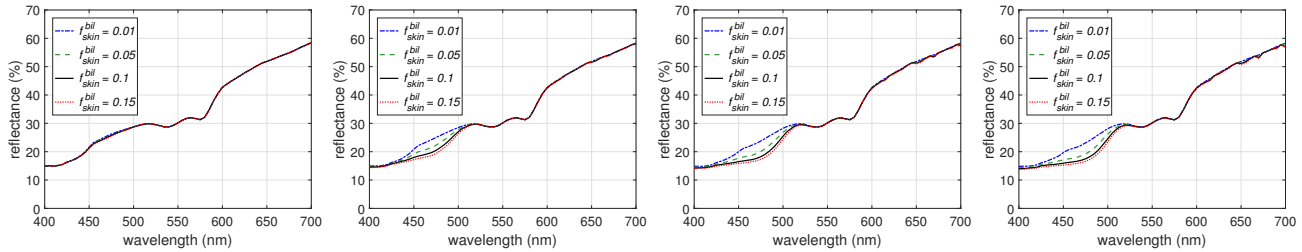

Fig. 5. Graphs depicting reflectance changes due to variations in extravascular bilirubin content, which is given by the product of f^{bil}_{skin} (bilirubin transference factor) by c^{bil}_{blood} (concentration of intravascular bilirubin). From left to right, c^{bil}_{blood} equal to 0.003, 0.071, 0.161 and 0.223 g/L, respectively.

Fig. 6. Skin swatches obtained using the reflectance curves provided in Fig. 5. From top to bottom rows, f^{skin}_{bil} varies from 0.01, 0.05, 0.1 and 0.15, respectively. From left to right, c^{bil}_{blood} varies from 0.003, 0.071, 0.161 and 0.223 g/L, respectively.

as the amount of bilirubin increases, going from a concave down to increasingly accentuated concave up shapes. This convergence trend suggests that the selected value for f^{bil}_{skin} may be close to the actual upper bound of this parameter.

Accordingly, the skin swatches depicted in Fig. 8, which were obtained considering the reflectance curves depicted in Fig. 7 (left), show a more pronounced yellow-tinted appearance. This is again corroborated by the CIELAB ΔE^*_{ab} differences computed for these swatches with respect to the baseline swatch presented in Fig. 2 (bottom right): 0.77, 9.22, 12.14, and 13.07 (from the leftmost to the rightmost swatch). These differences are higher than the ones computed for the previous cases. However, the differences computed for successive pairs of swatches, namely 8.51, 2.92 and 1.1067 (from the leftmost to the rightmost pair), are lower than their counterparts computed for those cases. This reinforces the inference that the visual assessment of jaundice becomes increasingly unsuitable for the differentiation and monitoring of variable degrees of hyperbilirubinemia severity as the extravascular bilirubin contents reach excessively high levels.

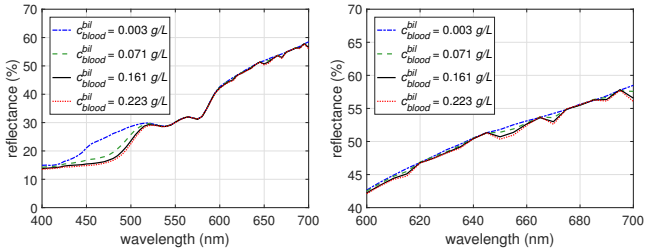

Fig. 7. Graphs depicting reflectance changes due to variations in the extravascular bilirubin content with the bilirubin transference factor (f^{bil}_{skin}) set to 0.2 and considering the four selected values for c^{bil}_{blood} (intravascular bilirubin concentration). Left: full spectral range. Right: zoom-in plot.

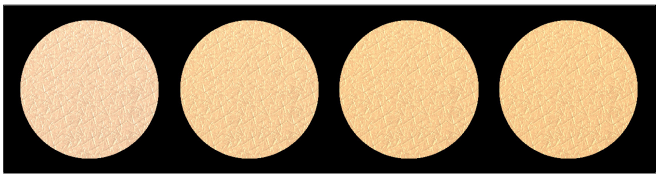

Fig. 8. Skin swatches obtained using the reflectance curves provided in Fig. 7. From left to right, c^{bil}_{blood} varies from 0.003, 0.071, 0.161 and 0.223 g/L, respectively.

Our experimental results suggest that a more appropriate approach to differentiate and monitor variable degrees of hyperbilirubinemia severity may lie on the detection of the optical features (reflectance dropping points) appearing in the red region. As it can be observed in the graphs presented in Fig. 5, when the blood bilirubin concentration reached an excessive level (0.161 g/L), these features started to become noticeable. In our experiments, these features appear around 650, 670 and 700 nm as highlighted in the zoom-in plot presented in Fig. 7 (right). These wavelengths correspond to the peaks in the red region of the bilirubin absorption spectrum considered in this investigation (Fig. 1 (right)). Since this absorption data was obtained under *in vitro* conditions [11], [12], spectral shifts in the position of these peaks may be expected under *in vivo* conditions. Nonetheless, the detection of these features may lead to hyperbilirubinemia screening protocols with a higher effectiveness/cost ratio than those currently employed at clinical settings, notably to support the point of care diagnosis of life-threatening pathologies associated with this medical condition.

IV. Concluding Remarks

Although the jaundice appearance of human skin may serve as an clinical indicator that a patient may be sub-

jected to hyperbilirubinemia, it has a limited applicability with respect to the differentiation of variable degrees of severity of this medical condition. Our findings indicate that the use of additional reflectance readings taken at specific wavelengths in the red region of the spectrum may lead to more reliable noninvasive protocols to differentiate and monitor high degrees of hyperbilirubinemia severity.

During our investigation, another key aspect related to the noninvasive assessment of hyperbilirubinemia was highlighted, namely the relatively high impact of the bilirubin transference factor on reflectance changes. Consequently, future efforts toward improving the reliability of transcutaneous estimations of intravascular and extravascular bilirubin contents should include a more precise quantification of this factor. This task, in turn, will likely require the pairing of traditional "wet" laboratory experiments with predictive computational simulations.

REFERENCES

[1] K.M. Van de Graaff, *Human Anatomy*, W. C. Brown Publishers, Dubuque, IO, USA, 4th edition, 1995.

[2] J. Fevery, "Bilirubin in clinical practice: A review," *Liver Int.l*, pp. 592–605, 2008.

[3] S.D. Zucker, P.S. Horn, and K.E. Sherman, "Serum bilirubin levels in the US population: Gender effect and inverse correlation with colorectal cancer," *Hepatology*, vol. 40, no. 4, pp. 827–835, 2004.

[4] F. Groenendaal, J. van der Grond, and L.S. de Vries, "Cerebral metabolism in severe neonatal hyperbilirubinemia," *Pediatrics*, vol. 114, no. 1, pp. 291–294, 2004.

[5] R.P. Wennberg, C.E. Ahlfors, V.K. Bhutani, L.H. Johnson, and S.M. Shapiro, "Toward understanding kernicterus: A challenge to improve the management of jaundice newborns," *Pediatrics*, vol. 117, no. 2, pp. 474–485, 2006.

[6] C.P. Strassburg, "Hyperbilirubinemia syndromes (Gilbert-Meulengracht, Crigler-Najjar, Dubin-Johnson, and Rotor syndrome," *Best Pract. Res. Cl. Ga.*, vol. 24, pp. 555–571, 2010.

[7] J. Moan, "Visible light and UV radiation," in *Radiation at home, outdoors and in the workplace*, D. Brune, B.R.R. Persson, and R. Pääkkönen, Eds. 2001, pp. 69–85, Scandinavian Science Publisher.

[8] A. Knudsen and R. Brodersen, "Skin color and bilirubin in neonates," *Archives of Diseases in Childhood*, pp. 605–609, 1989.

[9] H. Özkan, H. Ören, N. Duman, and M. Duman, "Dermal bilirubin kinetics during phototherapy in term neonates," *Acta Paediatr.*, vol. 92, pp. 577–581, 2003.

[10] V. Narendran W.L. Pickens, M.O. Visscher, and S.B. Hoath, "Neuroprotective core measure 6: Protecting skin- neuroprotective care in the newborn: does skin protect the immature brain from hyperbilirubinemia?," *Newborn & Infant Nurs. Rev.*, vol. 15, pp. 124–127, 2015.

[11] S.A. Prahl, "PhotochemCAD spectra by category," Tech. Rep., Oregon Medical Laser Center, 2001.

[12] H. Du, R.A. Fuh, J. Li, A. Corkan, and J.S. Lindsey, "PhotochemCAD: A computer aided design and research tool in photochemistry," *Photochemistry and Photobiology*, vol. 68, no. 2, pp. 142–142, 1998.

[13] R.E. Hannemann, D.P. Dewitt, E.J. Hanley, R.L. Schreiner, and P. Bonderman, "Determination of serum bilirubin by skin reflectance," *Pediat. Res.*, vol. 13, pp. 1326–1329, 1979.

[14] C.J. Kapoor and C.R.K. Murti, "Role of human skin in the photodecomposition of bilirubin," *Biochem. J.*, vol. 142, pp. 567–573, 1974.

[15] K. Grohmann, M. Roser, B. Rolinski, I. Kadow, C. Müller, A. Goerlach-Graw, M. Nauck, and H. Küster, "Bilirubin measurement for neonates: comparison of 9 frequently used methods," *Pediatrics*, vol. 117, no. 4, pp. 1174–1183, 2006.

[16] T. Karen, H.U. Bucher, and J. Fauchére, "Comparison of a new transcutaneous bilirubinometer (Bilimed) with serum bilirubin measurements in preterm and full-term infants," *BMC Pediatrics*, vol. 9, no. 70, pp. 1–7, 2009.

[17] P. Szabo, M. Wolf, H.U. Bucher, D. Haensse, J.C. Fauchére, and R. Arlettaz, "Assessment of jaundice in preterm neonates: comparison between clinical assessment, two transcutaneous bilirubinometers and serum bilirubin values," *Acta Paediatr.*, vol. 93, pp. 1491–1495, 2004.

[18] N. Bosschaart, J.H. Kok, A.M. Newsum, D.M. Ouweneel, R. Mentink, T.G. Van Leeuwen, and M.C.G. Aalders, "Limitations and opportunities of transcutaneous bilirubin measurements," *Pediatrics*, vol. 129, no. 4, pp. 689–694, 2012.

[19] S.N. El-Beshbishi, K.E. Shattuck, A.A. Mohammad, and J.R. Petersen, "Hyperbilirubinemia and transcutaneous bilirubinometry," *Clinical Chemistry*, vol. 5, no. 7, pp. 1280–1287, 2009.

[20] B.G. Harbrecht, M.R. Rsengart, K. Bubauskas, M.S. Zenati, J.W. Mrsh Jr., and D.A. Geller, "Assessment of transcutaneous bilirubinometry in hospitalized adults," *J. Am. Coll. Surg.*, vol. 206, no. 6, pp. 1129–1136, 2008.

[21] J.A.D. Atencio, S.L. Jacques, and S.V. Montiel, "Monte Carlo modeling of light propagation in neonatal skin," in *Applications of Monte Carlo methods in biology, medicine and other fields of science*, C.J. Mode, Ed. 2011, pp. 297–314, Intech.

[22] T. Hoang, S. Khan, L. Ortiz, and C.H. Lee, "Neonatal jaundice - Its mathematical model and treatments," *Rose-Hulman Undegraduate Mathematics Journal*, vol. 5, no. 1, pp. 1–16, 2004.

[23] T.F. Chen, G.V.G. Baranoski, B.W. Kimmel, and E. Miranda, "Hyperspectral modeling of skin appearance," *ACM Trans. Graph.*, vol. 34, no. 3, pp. 31:1–14, 2015.

[24] G.V.G. Baranoski, A. Dey, and T.F. Chen, "Assessing the sensitivity of human skin hyperspectral responses to increasing anemia severity levels," *J. Biomed. Opt.*, vol. 9, no. 20, pp. 095002–1–14, 2015.

[25] G.V.G Baranoski, S.R. van Leeuwen, and T.F. Chen, "On the detection of peripheral cyanosis in individuals with distinct levels of cutaneous pigmentation," in *39th Annual International Conference of the IEEE Engineering in Medicine and Biology Society (EMBC)*, Jeju Island, South Korea, August 2017, pp. 4260–4264.

[26] S.R. van Leeuwen and G.V.G Baranoski, "Elucidating the contribution of Rayleigh scattering to the bluish appearance of veins," *J. Biomed. Opt.*, vol. 23, no. 2, pp. 025001–1–17, 2018.

[27] G.V.G. Baranoski, J.G. Rokne, and G. Xu, "Virtual spectrophotometric measurements for biologically and physically-based rendering," *The Visual Computer*, vol. 17, no. 8, pp. 506–518, 2001.

[28] Natural Phenomena Simulation Group (NPSG), *Run HyLIoS Online*, School of Computer Science, University of Waterloo, Ontario, Canada, 2017, http://www.npsg.uwaterloo.ca/models/hyliosEx.php.

[29] G.V.G. Baranoski, T. Dimson, T.F. Chen, B. Kimmel, D. Yim, and E. Miranda, "Rapid dissemination of light transport models on the web," *IEEE Comput. Graph.*, vol. 32, pp. 10–15, 2012.

[30] NPSG, *Human Skin Data*, Natural Phenomena Simulation Group (NPSG), School of Computer Science, University of Waterloo, Ontario, Canada, 2014, http://www.npsg.uwaterloo.ca/data/skin.php.

[31] M.J. Vrhel, R. Gershon, and L.S. Iwan, "Measurement and analysis of object reflectance spectra," *Color Research and Application*, vol. 19, no. 1, pp. 4–9, 1994.

[32] World Health Organization, "Haemoglobin concentrations for the diagnosis of anaemia and assessment of severity," in *VMNIS - Vitamin and Mineral Nutrition Information System*, Geneva, Switzerland, 2011, pp. 1–6, WHO/NMH/NHD/MnM/11.1.

[33] R.L. Hayes and G.P. Rofnan, "The ultrastructure of skin in progressive sclerosis (scleroderma) I. dermal collagen fibers," *American Journal of Pathology*, vol. 63, no. 3, pp. 433–440, 1971.

[34] V.K. Bhutani, G.R. Gourley, S. Adler, B. Kreamer, C. Dalin, and L.H. Johnson, "Noninvasive measurement of total serum bilirubin in a multiracial predischarge newborn population to assess the risk of severe hyperbilirubinemia," *Pediatrics*, vol. 106, no. 2, pp. 1–9, 2000.

[35] M. Meinke, G. Müller, M. Friebel, and J. Helfmann, "Optical properties of platelets and blood plasma and their influence on the optical behavior of whole blood in the visible to near infrared wavelength range," *J. Biomed. Opt.*, vol. 12, no. 1, pp. 014024–1–9, 2007.

[36] R.W.G. Hunt, *Measuring Colour*, Ellis Horwood Limited, Chichester, England, 2nd edition, 1991.

[37] G.V.G. Baranoski and A. Krishnaswamy, *Light & Skin Interactions: Simulations for Computer Graphics Applications*, Morgan Kaufmann/Elsevier, Burlington, MA, USA, 2010.

[38] M. Stokes, M.D. Fairchild, and R.S. Berns, "Precision requirements for digital color reproduction," *ACM Trans. Graph.*, vol. 11, no. 4, pp. 406–422, 1992.

[39] D.H. Brainard, "Color appearance and color difference specification," *The Science of Color*, vol. 2, pp. 191–216, 2003.

[40] M. Mahy, L. Van Eycken, and A. Oosterlinck, "Evaluation of uniform color spaces developed after the adoption of CIELAB and CIELUV," *Color Research and Application*, vol. 19, no. 2, pp. 105–121, 1994.